Supplemental Table 1. Correlation between tumor grade and subcellular localization of PLAC8 on CRC TMA.

Tumor Grade	Total Cases	Membrane	Cytosol
I&II	62	45%	4%
III	22	50%	32%
Total	84	46%	11%

Statistic	Df	Chi-square	*P* value
Value	2	14.0223	0.0009

Df, Degrees of freedom

Supplemental Table 2. shRNA information (Sigma-Aldrich).

Gene	Catalogue #
PLAC8 sh1	TRCN0000133820
PLAC8 sh2	TRCN0000133929
ERK2 sh1	TRCN0000342295
ERK2 sh2	TRCN0000342296
ERK2 sh3	TRCN0000342297
ERK2 sh4	TRCN0000196392
ERK1 sh1	TRCN0000195323
ERK1 sh2	TRCN0000219700
Scrambled control	SHC005

Supplemental Table 3. Yeast two-hybrid analysis of interaction between PLAC8 and DUSP6.

Transformant		Growth on agar plates lacking		
GAL4AD-fusion protein	GAL4BD-fusion protein	AHLW	HLW	LW
GAL4AD	-	-	-	-
-	GAL4BD	-	-	-
GAL4AD-PLAC8	-	-	-	-
-	GAL4BD-DUSP6	-	-	-
GAL4AD-PLAC8	GAL4BD	-	+	+
GAL4AD	GAL4BD-DUSP6	-	-	+
GAL4AD-PLAC8	GAL4BD-DUSP6	+	+	+

AHLW: alanine, histidine, leucine, tryptophan; HLW: histidine, leucine, tryptophan; LW: leucine, tryptophan.

Supplemental Table 4. Antibodies used for immunoblotting, immunofluorescence and immunohistochemistry.

Antibody	Company	Catalogue #
PLAC8	Sigma-Aldrich	HPA040465
CDH1 (C-terminus)	BD Transduction Labs	610181
CDH1 (C-terminus)	Abcam	Ab40772
CDH1 (N-terminus)	LSBio	LS-B7125
Cdh1 (zebrafish)	(1)	
CDH2	Cell Signaling Tech	4061
CDH3	BD Transduction	610227
ZEB1	Sigma	HPA027524
CTNND1	Dr. Albert Reynolds	
VIM	DAKO	M0725
OCLN (OCCLUDIN)	Invitrogen	33-1500
CLDN4 (CLAUDIN 4)	Invitrogen	90-0900
TRIC (TRICELLULIN)	Invitrogen	700191
ZO-1	Invitrogen	61-7300
ERK1/2	Cell Signaling Tech	9102S
p-ERK1/2	Cell Signaling Tech	9101S
AKT	Cell Signaling Tech	9272S
p-AKT(S473)	Cell Signaling Tech	9271S
SRC	Millipore	05-184
p-SRC(Y416)	Cell Signaling Tech	2101
ATCB (β-actin)	Sigma	A5316
TUBA(α-tubulin)	EMD Millipore	CP06
MDM2	R&D Systems	MAB1244
CBLL1(HAKAI)	Abcam	Ab91185
GFP	Invitrogen	A11122
FLAG (M2)	Sigma	F1804
HA (12CA5)	Roche Applied Science	11583816001

1. Babb, S.G., and Marrs, J.A. 2004. E-cadherin regulates cell movements and tissue formation in early zebrafish embryos. *Dev Dyn* 230:263-277.

Supplemental Table 5a. Primers used in qRT-PCR.

Gene	Forward primer sequence (5' to 3')	Reverse primer sequence (5' to 3')
CDH1	TGCTCTTGCTGTTTCTTCGG	TGCCCCATTCGTTCAAGTAG
CDH2	GGCAGTAAAATTGAGCCTGA	GGAGTTTTCTGGCAAGTTGA
CDH3	AAGATCTTCCCATCCAAACG	CTACAGCGAAGACACCCTCA
CDH11	CGGAATTCATTGTCAAGGTC	CCGAAAAATAGGGTTGTCCT
CDH17	ATGCAAGTTCTTTTGCCAAG	TGTGTCTCCCCTCAGTGAAT
VIM	TCCAAGTTTGCTGACCTCTC	TCAACGGCAAAGTTCTCTTC
ZEB1	GCACAACCAAGTGCAGAAGA	CATTTGCAGATTGAGGCTGA
OCLN	ATGACAAGCGGTTTTATCCA	CTCCAGCTCATCACAGGACT
AKT1	ACCTTTTCGACGCTTAACCT	TGGAGGGAAGGTTCCATATT
PLAC8	GTTTCACCATCTTGGTCAGG	CTGTAATTCCAGCACCTTGG
SNAI1	ACCCCACATCCTTCTCACTG	TACAAAAACCCACGCAGACA
SNAI2	CTTTTTCTTGCCCTCACTGC	GCTTCGGAGTGAAGAAATGC
TWIST1	GTCCGCAGTCTTACGAGGAG	CCAGCTTGAGGGTCTGAATC
TWIST2	GGGAGTGAGCACATTAGCAA	GGGCATGAGTACCCTTAGGA
ACTB	GGACTTCGAGCAAGAGATGG	AGCACTGTGTTGGCGTACAG

*All primers were purchased from RealtimePCR.com and first validated using standard curve method followed by melting curve before applying to experimental samples.

Supplemental Table 5b. Other primers used in the study.

Primer name	Forward primer sequence (5' to 3')	Reverse primer sequence (5' to 3')
PLAC8 cloning primer	GGAATGCAAGCTCAGGCGCCGGTG	TGGATCCGAAGATCTTGAAAGTACGCAT GGCT
VU44 genotyping primer	GGCTCAATATAACAGGCTCTGGGCAGATTC	CACTGGGGCTGATTCACGATTGCAC
plac8.1 cloning primer	TAATACGACTCACTATAGGCTCGAGTCATAATTTCAGCGTGCCGTTACTCTTTC	ATTTAGGTGACACTATACTCGAGTCATAATTTCAGCGTGCCGTTACTCTTTC
plac8.1-EGFP cloning primer	TAATACGACTCACTATAGGCTCGAGTCATAATTTCAGCGTGCCGTTACTCTTTC	GGACTAGTTAATTTCAGCGTGCCGTTACTCTTTC
plac8.1-EGFP mt2 primer	GCCAGTGACATGAACGAGGGCGGCTTGTGTGGTTTAGGC	GCCTAAACCACACAAGCCGCCCTCGTTC ATGTCACTGGC
plac8.1-EGFP mt3 primer	ATCGCCAGTGGCATGGGCGGGTG CTGCTTGTGTGG	CCACACAAGCAGCACCCGCCCATGCCA CTGGCGAT

Supplemental Table 6. Antibodies used for *MultiOmyx*, staining sequence, labeling and secondary antibody labeling

Antibody	Company	Catalogue #	Concentration	Labeling/ secondary detection	Staining round
PLAC8	Sigma-Aldrich	HPA040465	1:1000	Cy3-conjugated donkey anti-rabbit IgG secondary antibody	1
CDH1	Cell Signaling	3195BF	5 μg/ml	Cy5-conjugated	5
CDH3	BD Bioscience	610228	20 μg/ml	Cy5-conjugated	4
CK	Sigma	C1801	5 μg/ml	Cy7-conjugated	2
VIM	Cell Signaling	9856	1 μg/ml	Cy5-conjugated	3

Supplemental figures and supplemental figure legends

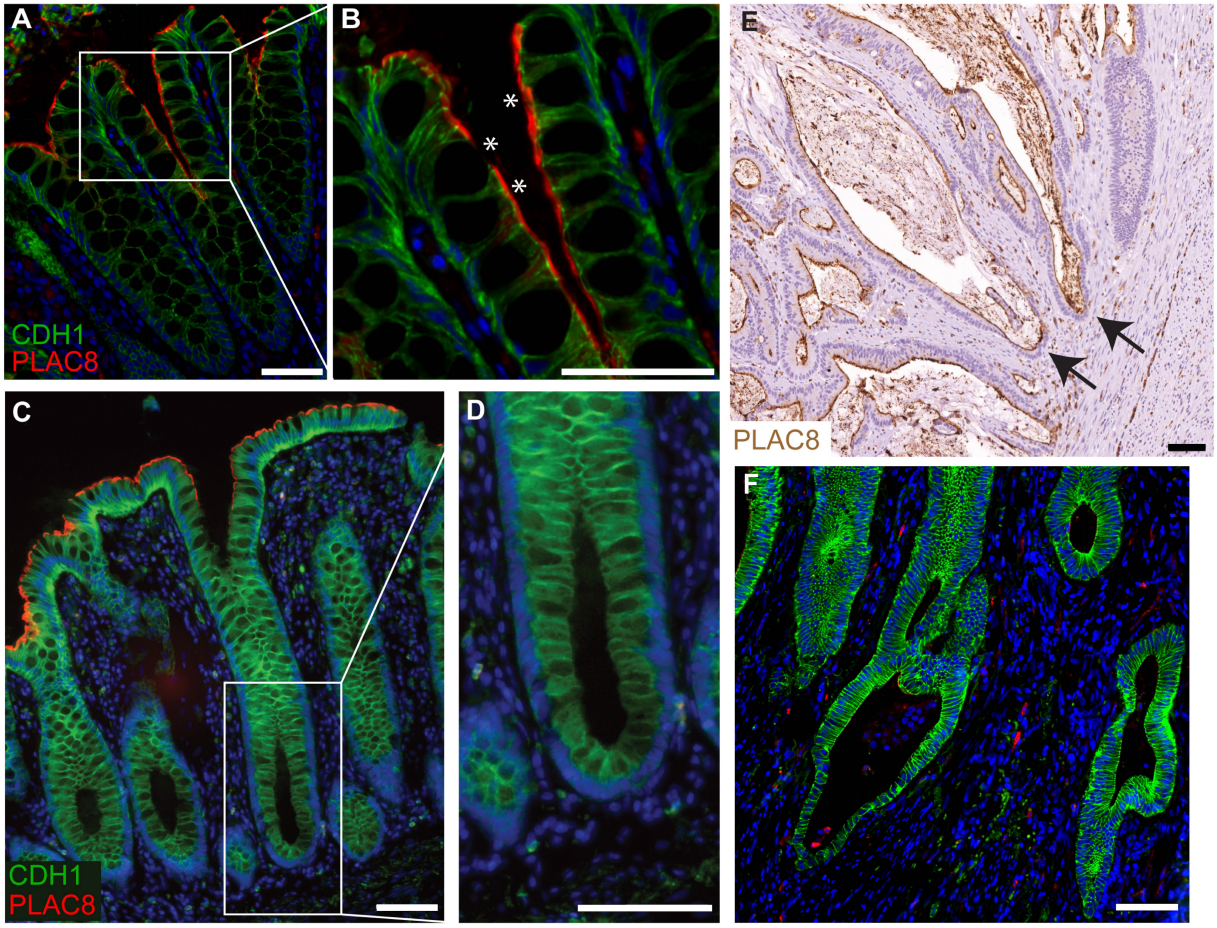

Supplemental Figure 1

PLAC8 immunofluorescence in normal and neoplastic human colon. (**A** and **B**) In normal colon, PLAC8 immunofluorescence (red) localizes to apical domain of both differentiated colonocytes and goblet cells. CDH1 immunofluorescence (green) was used to outline epithelia, and DAPI staining (blue) was used to label nuclei. Boxed region in (**A**) is magnified in (**B**) to show goblet cells (asterisks). (**C** and **D**) In normal colon, PLAC8 does not localize to bottom of crypts. (**E**) In a typical moderately differentiated colorectal adenocarcinoma, PLAC8 also localizes to apical domain, but immunoreactivity extends deeper into neoplastic crypts. (**F**) PLAC8 expression was absent in a subset of human colorectal adenocarcinomas. Scale bars: 100 μm.

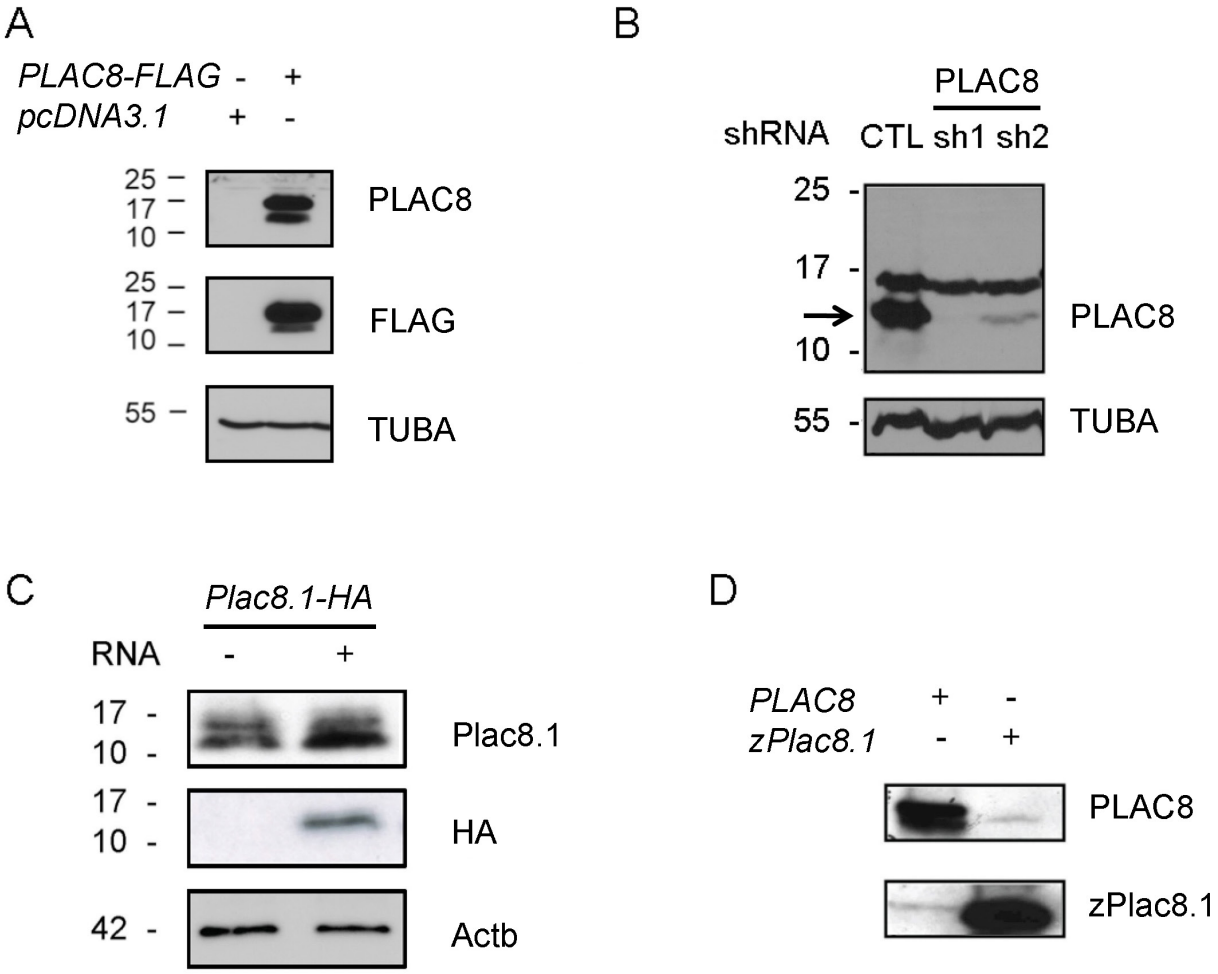

Supplemental Figure 2

Characterization of anti-PLAC8 antibodies. (**A**) FLAG-tagged *PLAC8* cDNA or control pcDNA3.1 vector were transfected into HEK293T cells. Both affinity-purified anti-PLAC8 antibody and anti-FLAG antibody recognized PLAC8-FLAG chimera. (**B**) Anti-PLAC8 antibody recognized endogenous PLAC8 protein (arrow) in SC cells cultured in 3D collagen. Decreased levels of endogenous PLAC8 protein by *PLAC8* shRNAs indicate specificity of anti-PLAC8 antibody. (**C**) A zebrafish Plac8.1-HA fusion protein was detected by both anti-Plac8.1 and anti-HA antibodies. (**D**) His-tagged human PLAC8 and His-tagged zebrafish Plac8.1 proteins were affinity purified from *E. coli* overexpressing corresponding proteins by nickel affinity chromatography, followed by immunoblotting with anti-human PLAC8 antibody or anti-zebrafish Plac8.1 antibody, respectively.

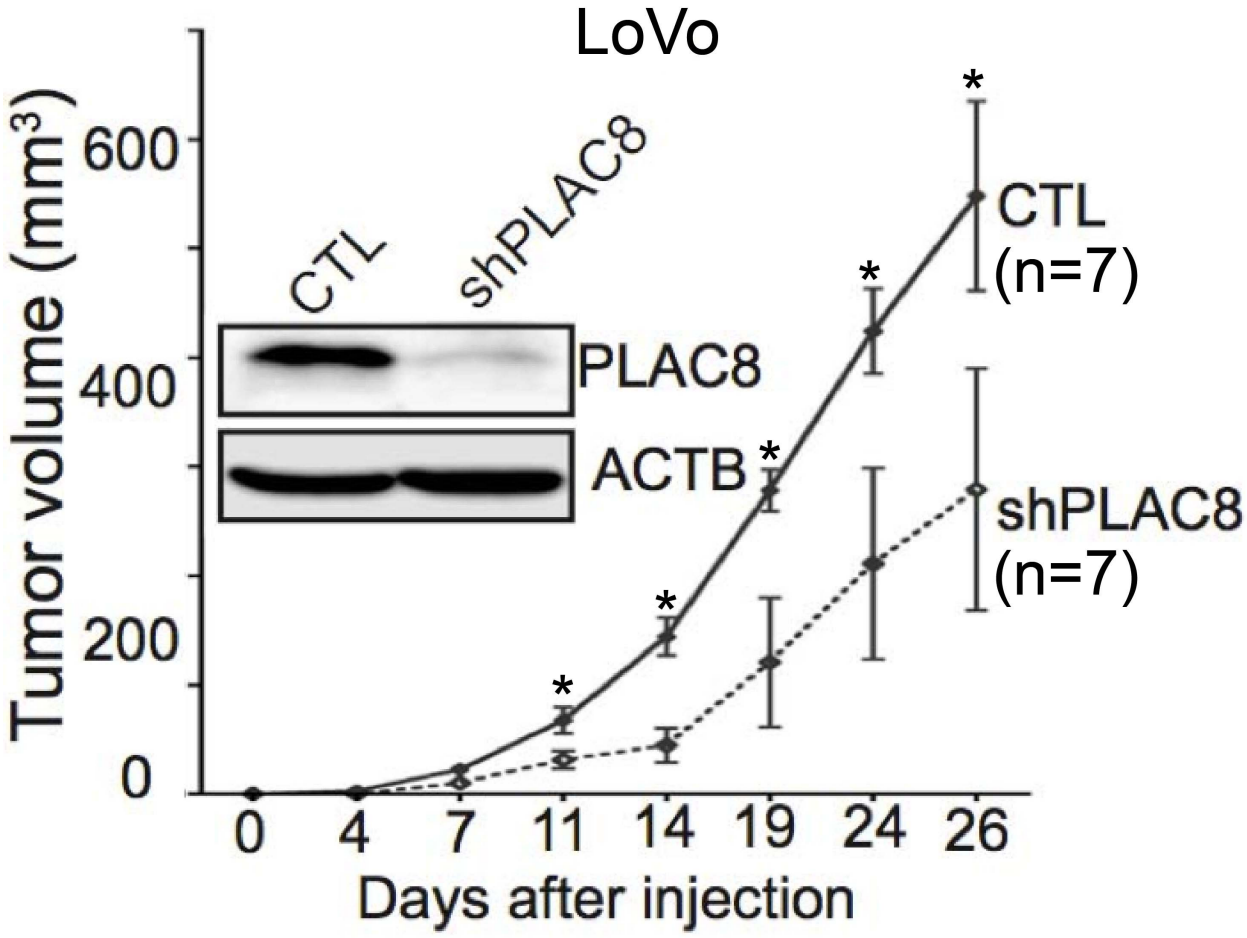

Supplemental Figure 3

Knockdown of endogenous PLAC8 in LoVo CRC cells significantly reduced tumor growth in xenografts as measured by tumor volume presented as mean ± SEM (*$P < 0.05$). This experiment was performed once.

A

```
zPlac8.1        ------MEVTSQP-----SAFHPQEFHSGLMSCCDDVGVCCCGLFCLPCMGCSIASDMNE 49
hPLAC8          MQAQAPVVVVTQPGVGPGPAPQNSNWQTGMCDCFSDCGVCLCGTFCFPCLGCQVAADMNE 60
                      : *.:**     .* : .::::*: .* .* *** ** **:**:**.:*:**** 

zPlac8.1        CCLCGLGMPMRSVYRTKYNIEGSMCNDWAATTFCFTCAACQLKRDIDIRKSNGTLKL    106
hPLAC8          CCLCGTSVAMRTLYRTRYGIPGSICDDYMATLCCPHCTLCQIKRDINRRRAMRTF--    115
                ***** .:.**::***:*.* **:*:*: **  *  *: **:****: *::  *:
```

B

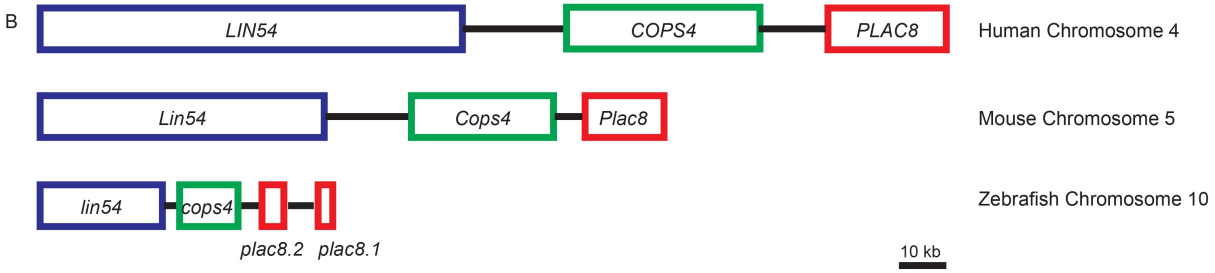

C

	Plac8.2	Human PLAC8	Mouse PLAC8
Plac8.1	75.5% 83.0%	44.4% 61.5%	43.9% 59.6%
Plac8.2	-	41.5% 55.9%	42.9% 58.0%
Human PLAC8	-	-	80.3% 85.5%

D

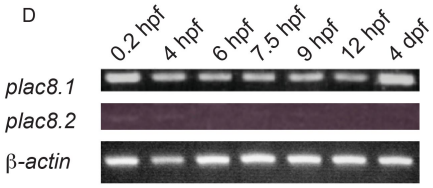

E

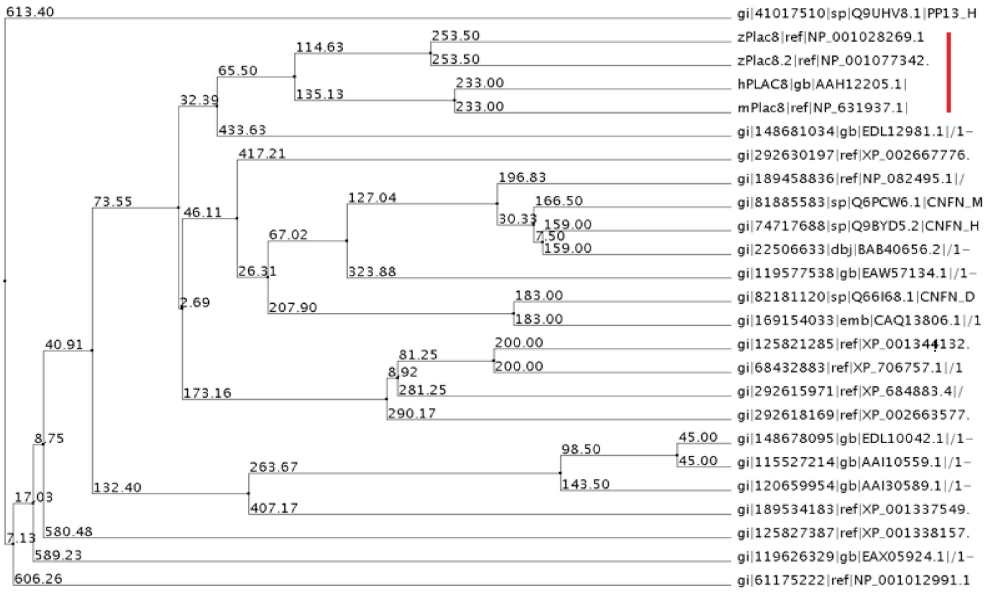

Supplemental Figure 4

Identification of zebrafish *plac8* homologs. (**A**) Amino acid sequence alignment of zebrafish Plac8.1 (zPlac8.1) and human PLAC8 (hPLAC8). Identical amino acid residues are denoted by "*"; conserved substitutions and semi-conserved substitutions are denoted by ":" and ".", respectively. (**B**) A schematic of gene arrangement of *Plac8* loci in humans, mouse, and zebrafish. (**C**) Comparison of amino acid sequences among zebrafish Plac8.1, Plac8.2 and mammalian PLAC8 proteins. The two numbers in each box denote identity (top) and similarity (bottom). (**D**) Zebrafish *plac8.1* and *plac8.2* expression was examined by RT-PCR from RNA extracted from zebrafish embryos at various developmental time points. (**E**) Phylogenetic analysis of Plac8 domain-containing proteins from human, mouse, and zebrafish shows that the four Plac8 proteins cluster together (marked by vertical red line).

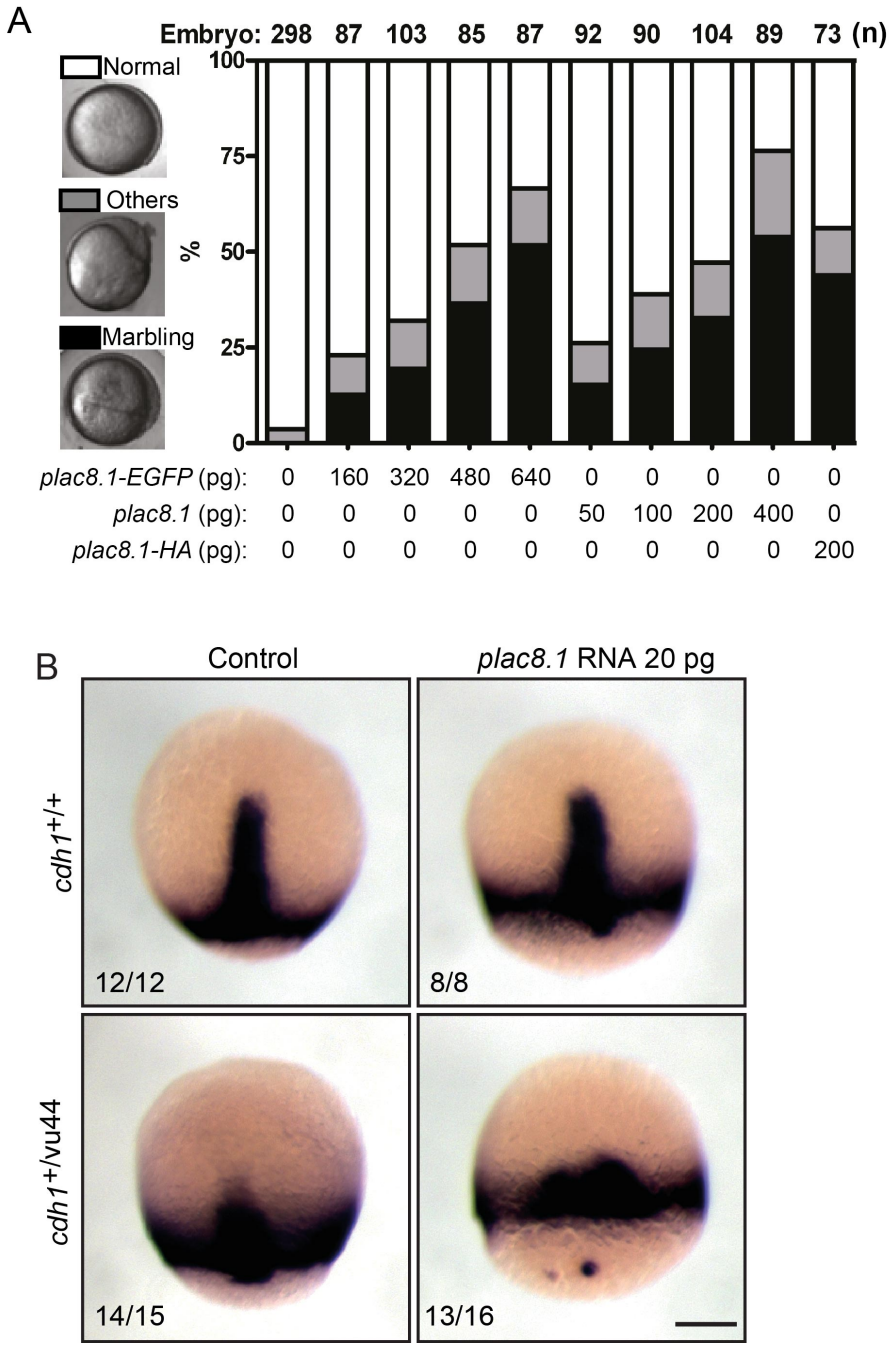

Supplemental Figure 5

Effect of Plac8.1 overexpression on zebrafish embryonic development. (**A**) Quantitation of percentage of normal embryos (normal, open bars), embryos showing the phenotype in Figure 4A (marbling, filled bars), or embryos showing other defects (others, gray bars). The total numbers of embryos are labeled on top of each column. Results from three independent injection experiments are plotted. The type and amount of synthetic RNA injected are labeled at bottom of plot. (**B**) Expression of low dose Plac8.1 exacerbates embryonic developmental defects in *cdh1*$^{+/vu44}$ embryos. Representative micrograph of *ntl* ISH in wild-type (top) or *cdh1*$^{+/vu44}$ embryos injected with 20 pg *plac8.1* RNA (bottom). DNA samples from embryos were extracted after ISH pictures were taken, followed by genotyping of the *cdh1* gene. The numbers of embryos are labeled in the lower left corner of each picture. Scale bar: 500 μm.

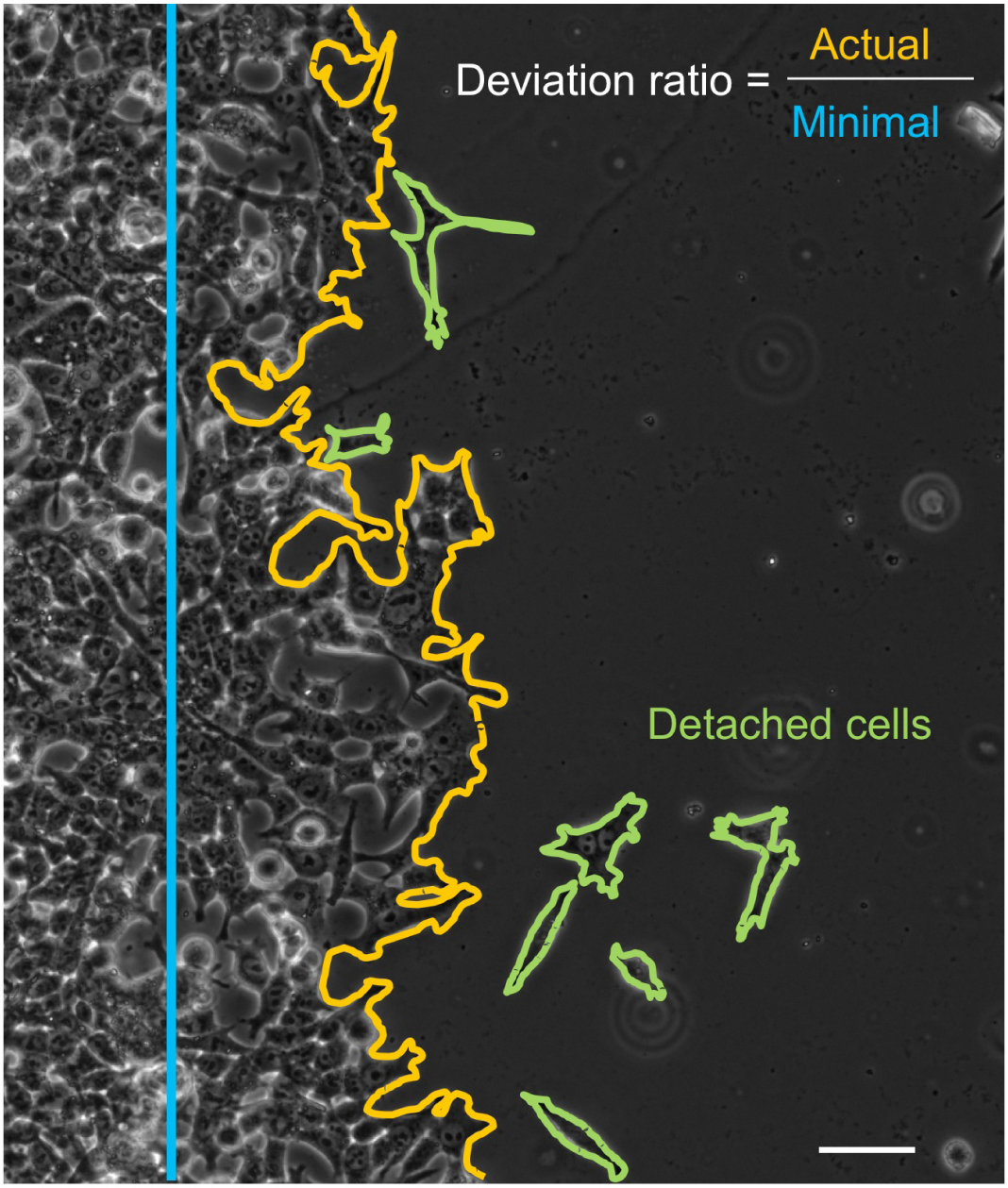

Supplemental Figure 6

Cell migration measurement. Blue line represents the start border after removing stencil. Yellow line outlines migratory edge of cell sheet at an experimental time point. Countable detached cells are illustrated in green hollows. Scale bar: 100 μm.

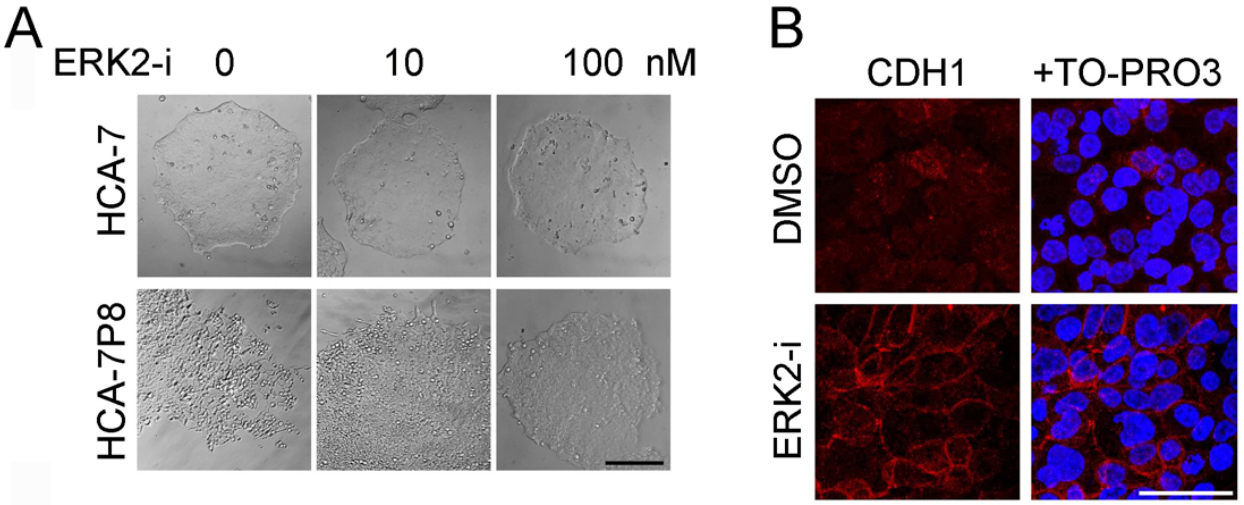

Supplemental Figure 7

ERK2 inhibition reverts EMT phenotypes in HCA-7P8 cells. (A) HCA-7P8 cells plated on cover slips were treated with ERK2-slective inhibitor, pyrazolylpyrrole, at a concentration of 10 or 100 nM for five days. Cell morphology was reverted to smooth-edged colonies as visualized by DIC microscopy. Scale bar: 500 μm. (B) Restoration of cell surface CDH1 immunofluorescence after exposure of HCA-7P8 cells to 100 nM ERK2 inhibitor for five days. Scale bar: 50 μm.

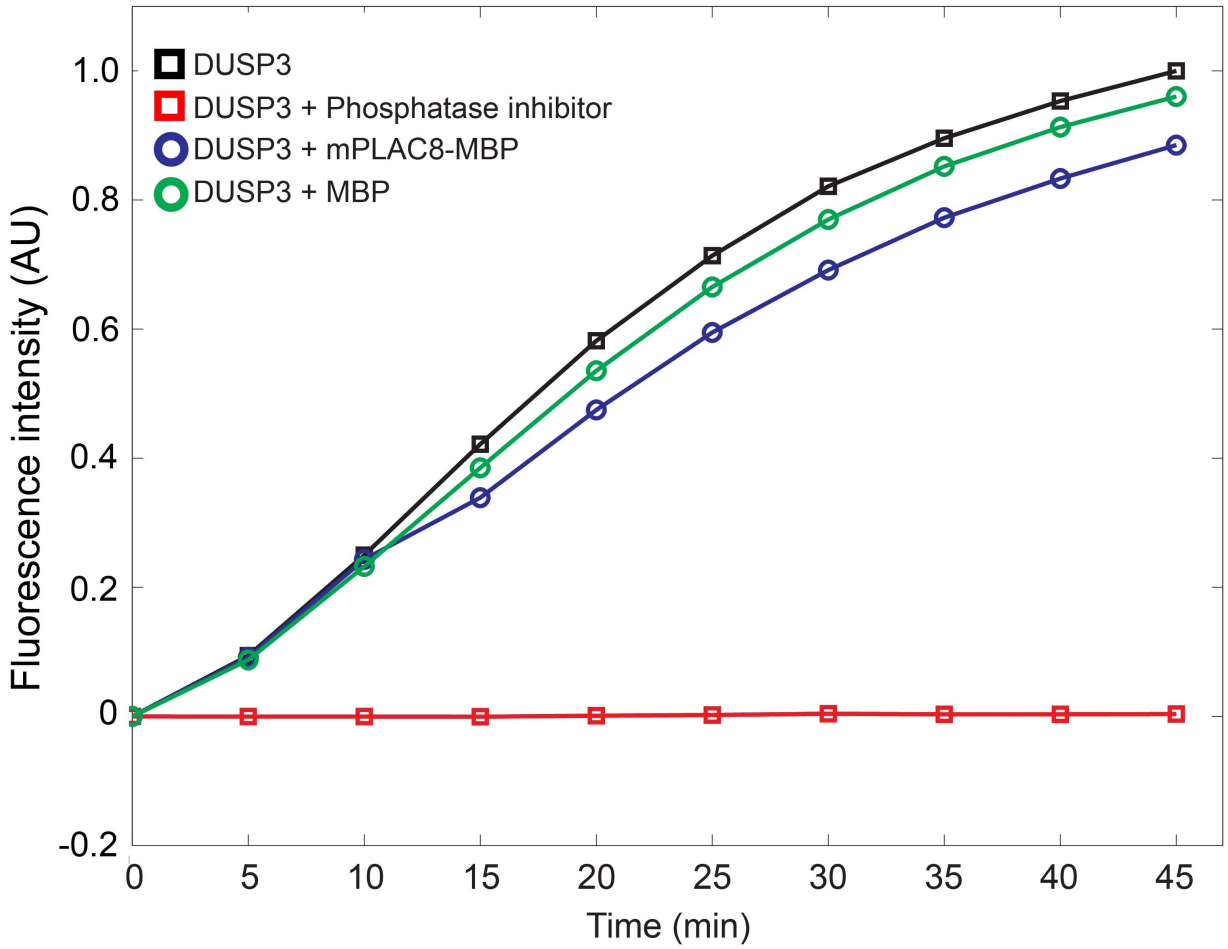

Supplemental Figure 8

PLAC8 does not inhibit DUSP3 phosphatase activity. Representative result of DUSP3 phosphatase activities measured by using 3-O-methylfluorescein phosphate as substrate (excitation 485 nm, emission 528 nm). Fluorescence intensity increased in control sample (black squares, DUSP3). Phosphatase inhibitor cocktail was added as a control to abolish the fluorescence intensity (red squares). In contrast to phosphatase inhibitor cocktail, addition of MBP (green circles) or MBP-mPLAC8 (blue circles) did not significantly affect fluorescence intensity.

A

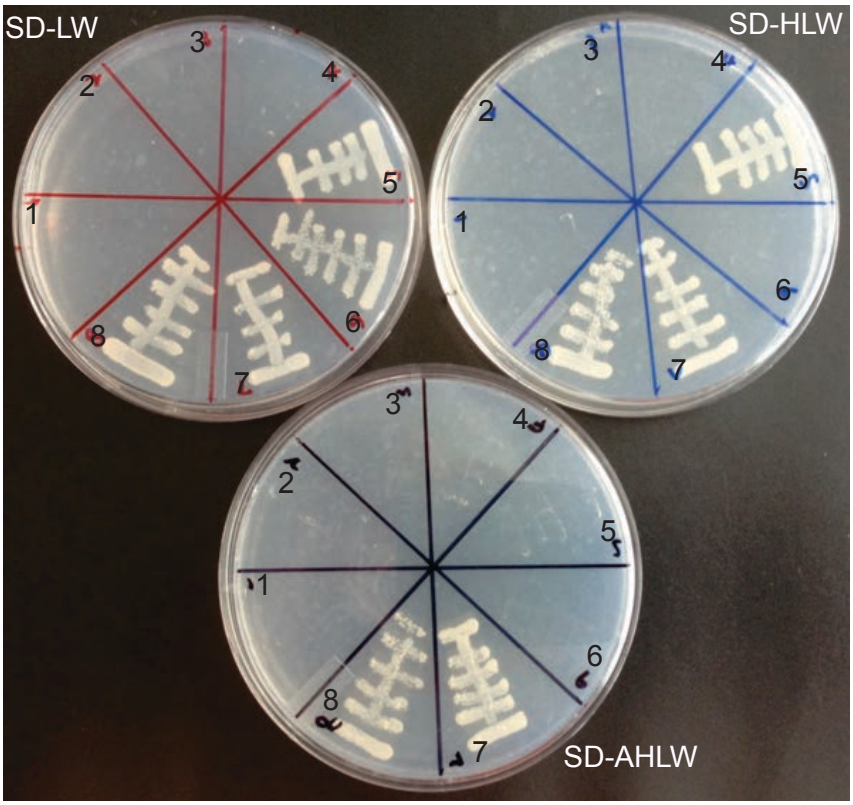

Supplemental Figure 9

Yeast two-hybrid analysis of PLAC8 and DUSP6 interaction. Representative plates of yeast two-hybrid using PLAC8 fusion to Gal4 protein activation domain (prey), and DUSP6 fusion to Gal4 DNA binding domain (bait). Only presence of both PLAC8 and DUSP6 resulted in yeast growth on medium lacking adenine, histidine, leucine and tryptophan (SD-AHLW). Medium lacking leucine and tryptophan (SD-LW) and medium lacking histidine, leucine and tryptophan (SD-HLW) were used as controls.

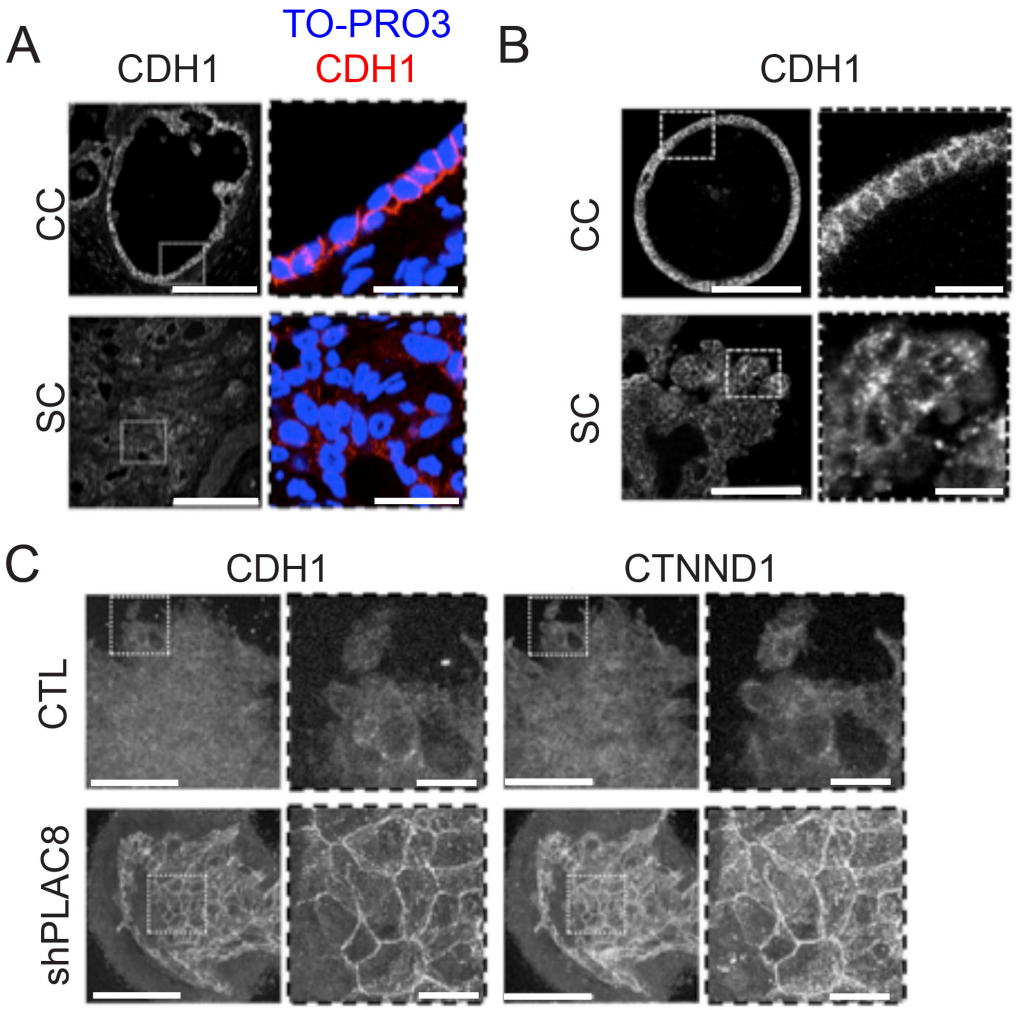

Supplemental Figure 10

Depletion of endogenous PLAC8 in SC cells restores cell surface CDH1 in xenografts and in 3D culture. (**A**) CC and SC cells were subcutaneously injected into athymic nude mice. After four weeks, CC cells formed glandular tumors with large cysts (top panel) with CDH1 (red) immunofluorescence observed at basolateral membrane. SC cells formed less differentiated tumors with reduced membranous and enhanced cytoplasmic CDH1 immunofluorescence. Boxed areas are magnified on right with DNA dye TO-PRO3. (**B**) In 3D collagen culture, CDH1 localized to basolateral plasma membrane of CC cells, whereas CDH1 was detected diffusely in cytoplasm of SC cells. Boxed areas are magnified on right. Scale bar: 100 μm; enlarged images: 20 μm. (**C**) SC cells were stably infected with PLAC8-specific shRNA (shPLAC8) or non-targeted control (CTL). In 3D collagen culture, both CDH1 and CTNND1 immunofluorescence were restored to the plasma membrane upon PLAC8 depletion from SC cells. Scale bars in enlarged images: 20 μm; other scale bars: 100 μm.

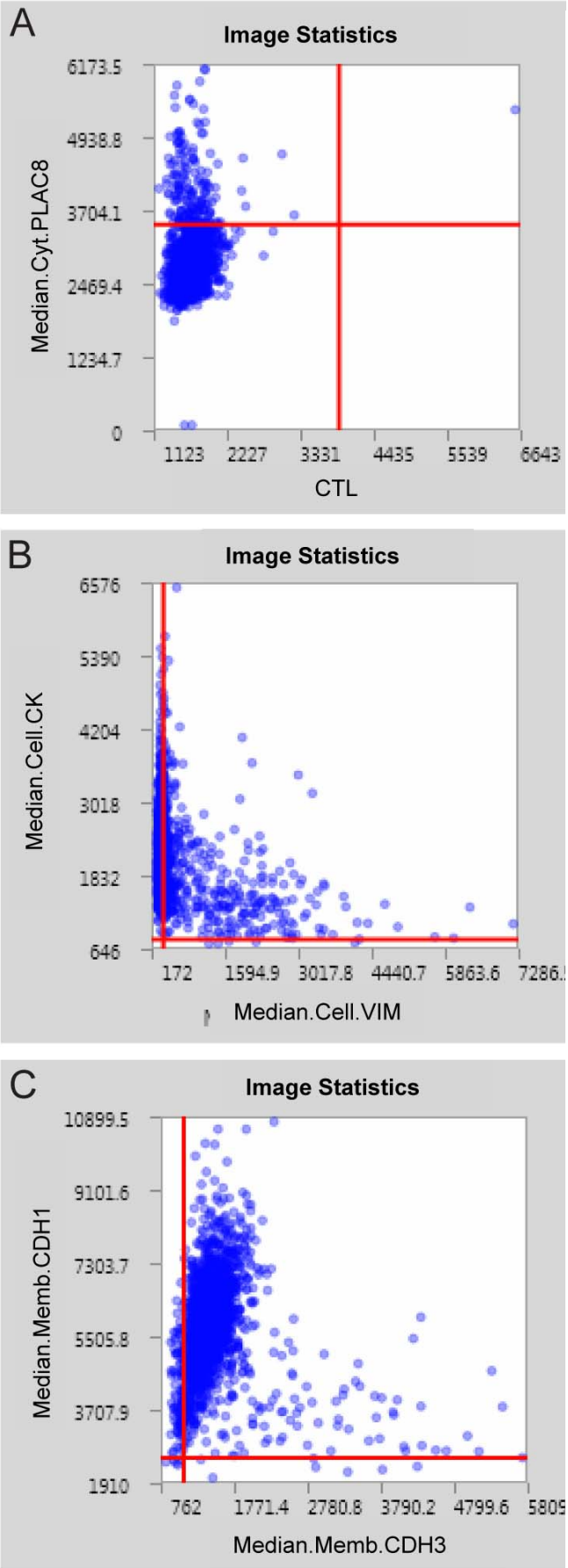

Supplemental Figure 11

Graphic depiction of pairwise coexpression for immunofluorescent staining intensities of different proteins within a cell. Each point on the plot represents a single cell present in Figure 10. Thresholds for cellular expression and localization of multiple markers were set by adjusting threshold bars such that cells in the original image are highlighted if expression was detected by visual inspection (not shown), thus allowing final thresholds to be set to include positive cells of interest. (A) Control graph for PLAC8 expression. $PLAC8^{+}$ cell threshold was set based on its cytoplasmic expression levels so that the top 10% of cells were included. The data are presented against a blank channel (X-axis), so that PLAC8 expression values can be properly determined alone. (B) CK and VIM thresholds were set to include all cells positive for either marker in the cytoplasm. The dot-plot analysis reveals a trend toward mutually exclusive expression of either CK or VIM, but generally not both, indicated by lack of double-positive cells in dot-plot. (C) CDH1 and CDH3 thresholds were set to include all cells positive for either marker on the membrane. The vast majority of cells express CDH1, while only some express CDH3. Very few cells express both markers.

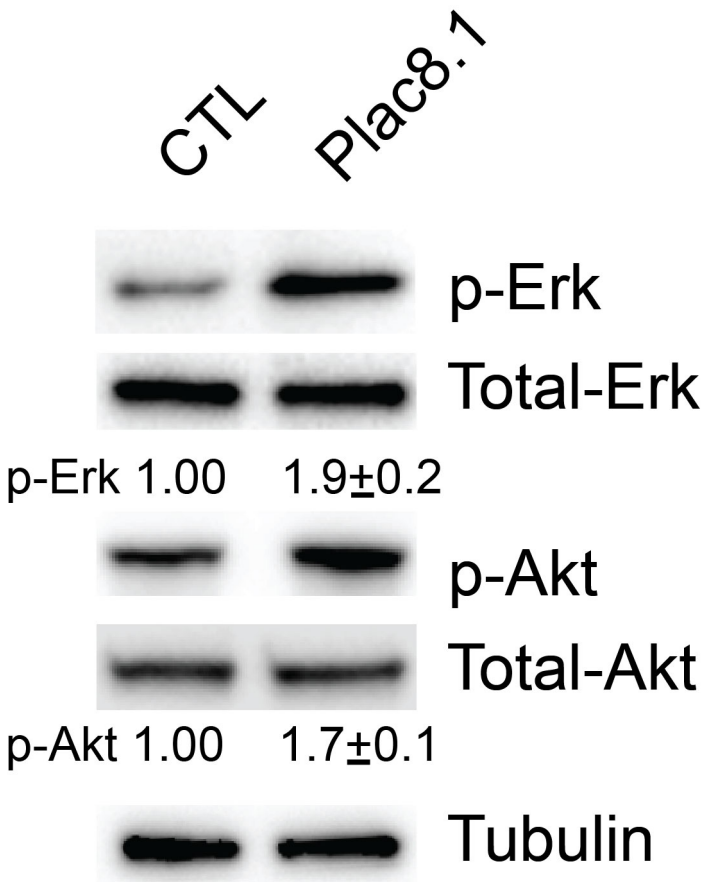

Supplemental Figure 12

Plac8.1 overexpression results in increased phosphorylation of Erk and Akt in zebrafish embryos. Representative immunoblotting showed increased Erk phosphorylation levels and Akt phosphorylation levels in Plac8.1-overexpressing zebrafish embryo compared to control. Average levels for pErk and pAkt were normalized to levels of tubulin, and are shown as mean ± SEM from at least three independent experiments.

Unedited gels for:

Excess PLAC8 promotes ERK2-dependent unconventional EMT in colon cancer

Cunxi Li[1†¶], Haiting Ma[2†], Yang Wang[1], Zheng Cao[1], Ramona Graves-Deal[1], Anne E. Powell[1], Alina Starchenko[3], Gregory D. Ayers[4], Mary Kay Washington[5], Vidya Kamath[6], Keyur Desai[6] Michael J. Gerdes[6], Lila Solnica-Krezel[2] and Robert J. Coffey[1,3,7*]

[1]Department of Medicine, Vanderbilt University Medical Center, Nashville, Tennessee, USA. [2]Department of Developmental Biology, Washington University School of Medicine, St. Louis, Missouri, USA. [3]Department of Cell and Developmental Biology, [4]Department of Statistics, and [5]Department of Pathology, Vanderbilt University Medical Center, Nashville, Tennessee, USA. [6]GE Global Research, Diagnostics and Biotechnology, One Research Circle, Niskayuna, New York, USA. [7]Department of Veterans Affairs Medical Center, Nashville, Tennessee, USA.

† Authorship note: Cunxi Li and Haiting Ma contributed equally to this work.

Conflict of interest: Vidya Kamath, Keyur Desai, and Michael J. Gerdes are affiliated with GE Global Research Center, Niskayuna, New York, USA, and are current employees of General Electric Company.

¶ Current address: Molecular Cytogenetics Laboratory, Beijing Jiaen Hospital Bldg.11, 29 Zhichun Road, Haidian District, Beijing, China.

*Address correspondence to:
Robert J. Coffey, MD
Epithelial Biology Center
10415 MRB IV
Vanderbilt University Medical Center
Nashville, TN 37232-0441
Phone: 615-343-6228; Fax: 615-343-1591
E-mail: robert.coffey@vanderbilt.edu.

Figure 2A PLAC8

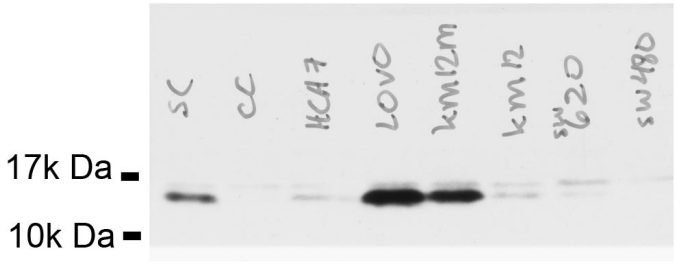

Figure 2A ACTB

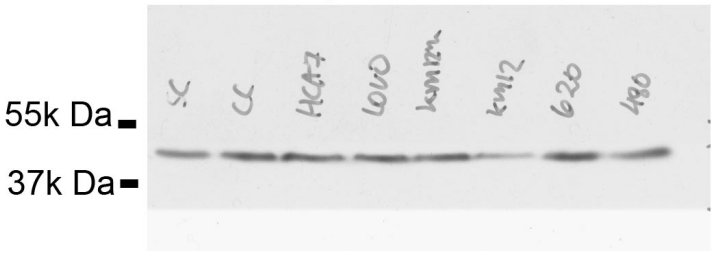

Figure 2C left panel PLAC8

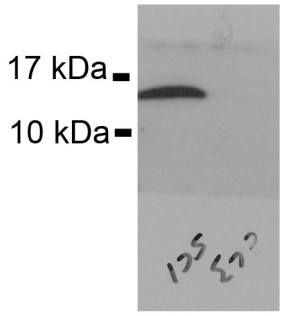

Figure 2C right panel PLAC8

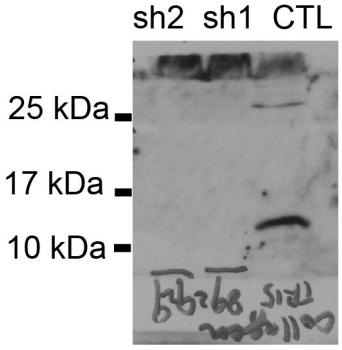

Figure 2D PLAC8

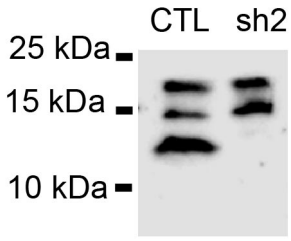

Figure 2C left panel ACTB

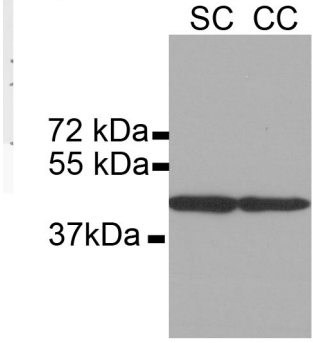

Figure 2C right panel ACTB

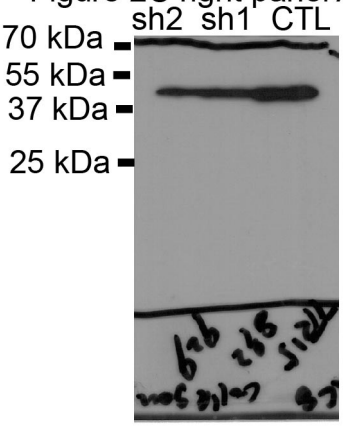

Figure 2D ACTB

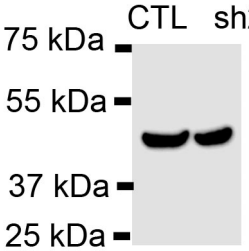

Figure 4H Cdh1

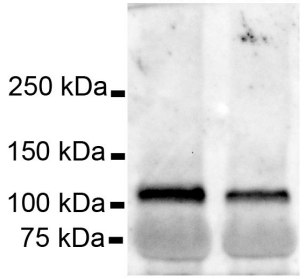

Figure 4H Actb

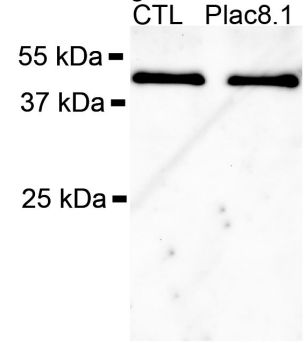

Figure 6B CDH1

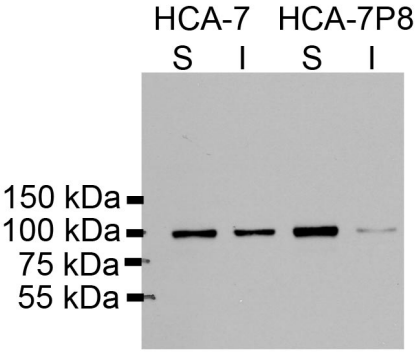

Figure 6B ACTB

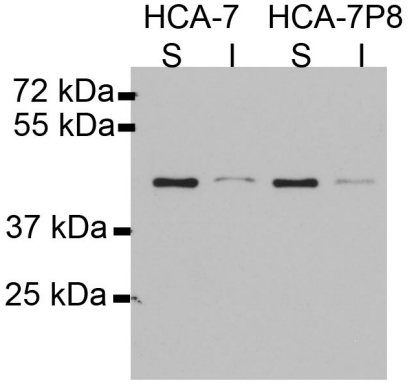

Figure 6B CDH3

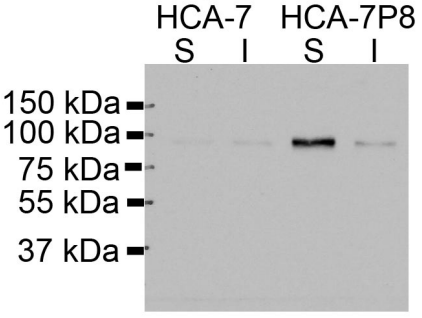

Figure 6B AKT

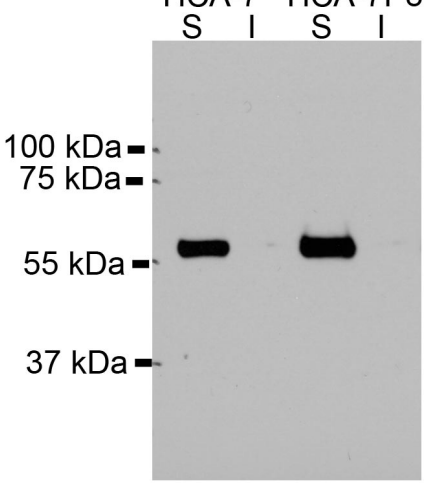

Figure 6C PLAC8

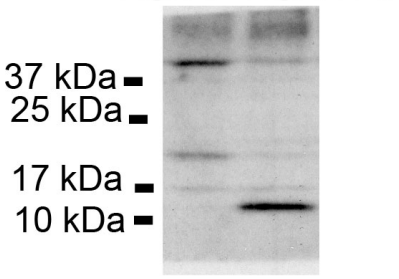

Figure 6C VIM

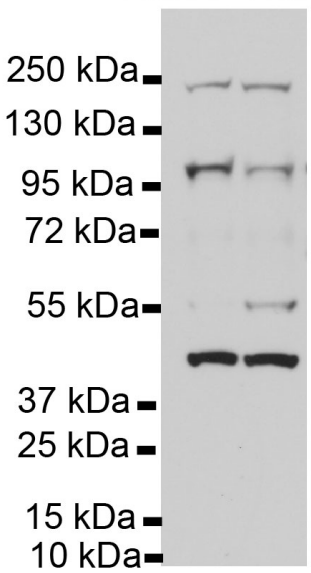

Figure 6C CDH3

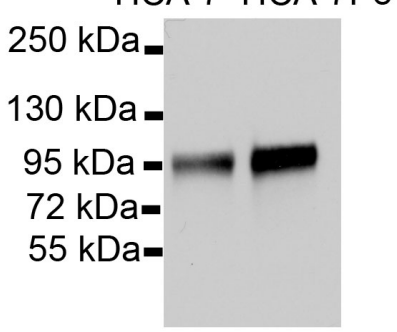

Figure 6C CDH1

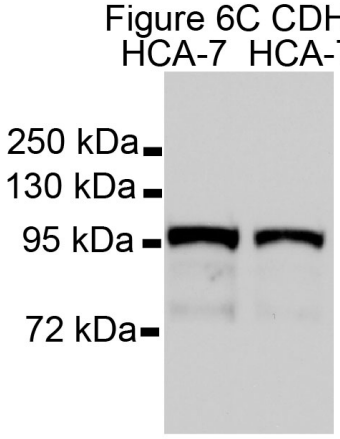

Figure 6C ACTB

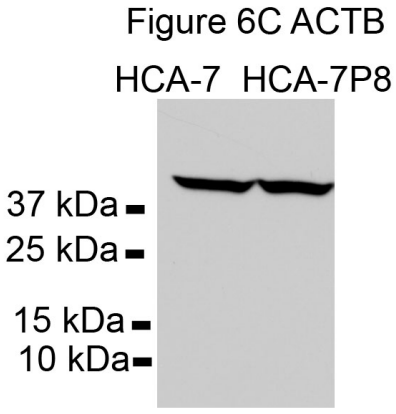

Figure 6C CTNND1

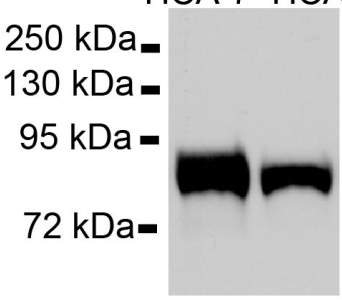

Figure 6C ZEB1

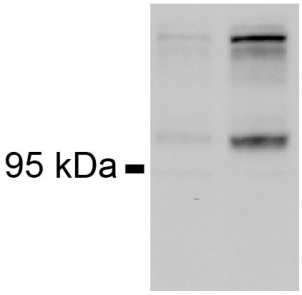

Figure 6D OCLN

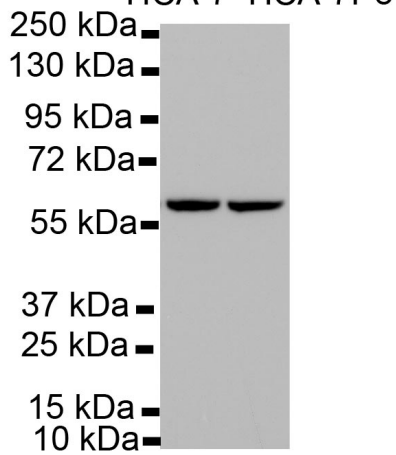

Figure 6D TRIC

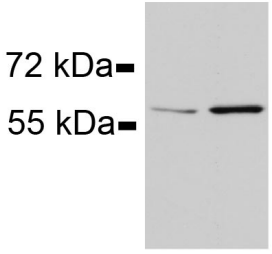

Figure 6D JAM-A

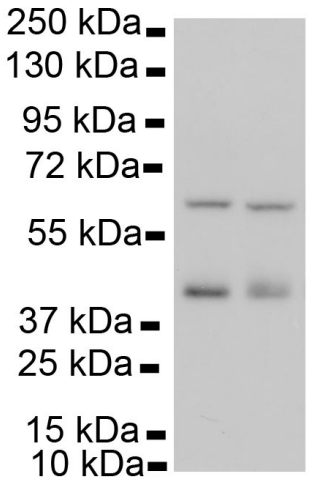

Figure 6D ZO-1

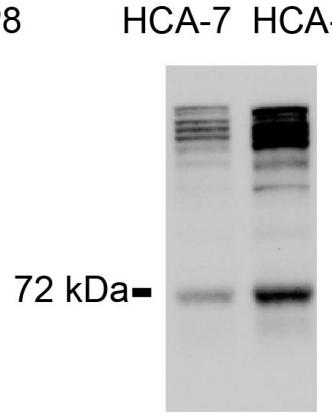

Figure 6D ACTB

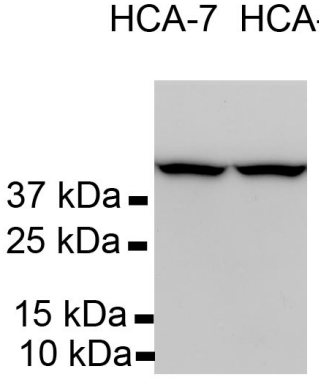

Figure 7A p-ERK1/2

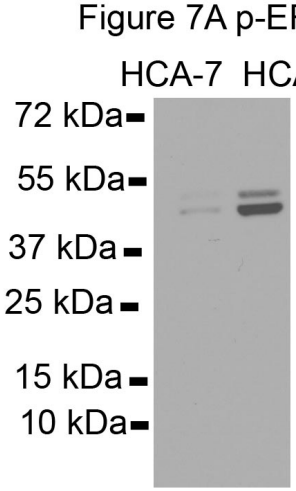

Figure 7A ERK1/2

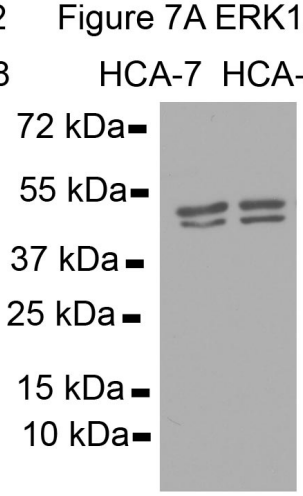

Figure 7A p-AKT

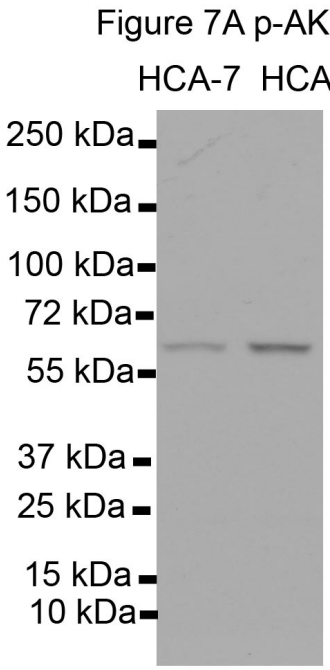

Figure 7A AKT

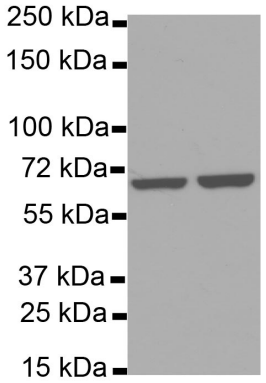

Figure 7A SRC

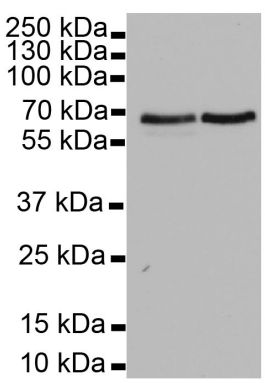

Figure 7A p-SRC

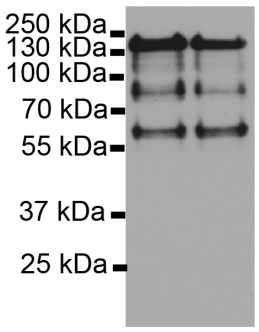

Figure 7A ACTB

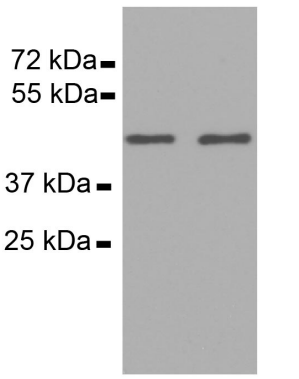

Figure 7B ERK1/2

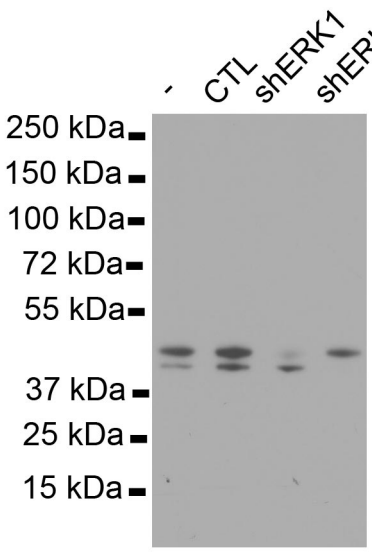

Figure 7B ACTB

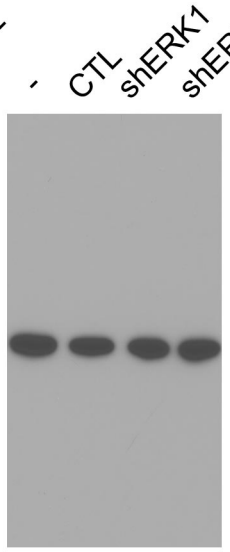

Figure 8B Myc

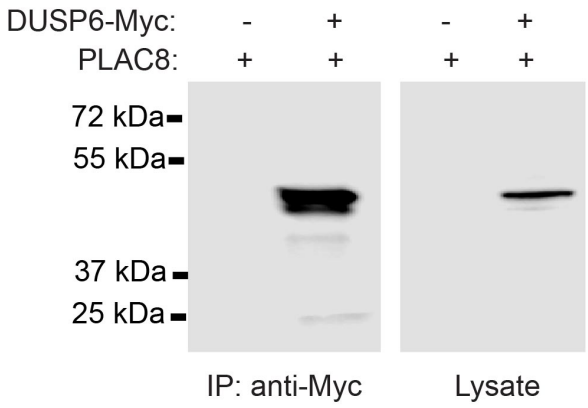

Figure 8B PLAC8

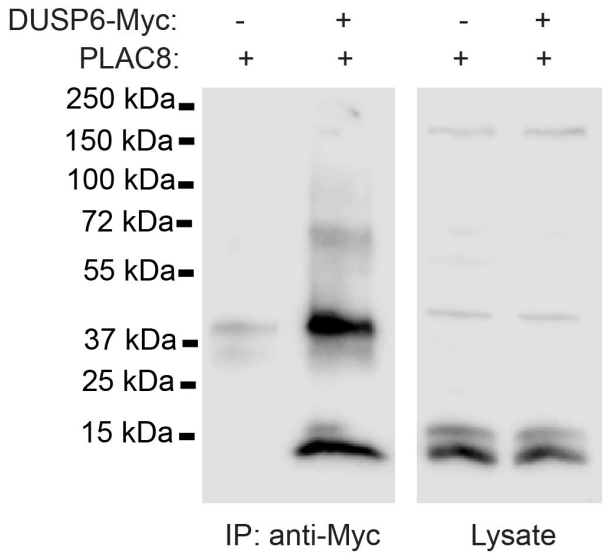

Figure 9B p-ERK1/2 Figure 9B ERK Figure 9B ACTB

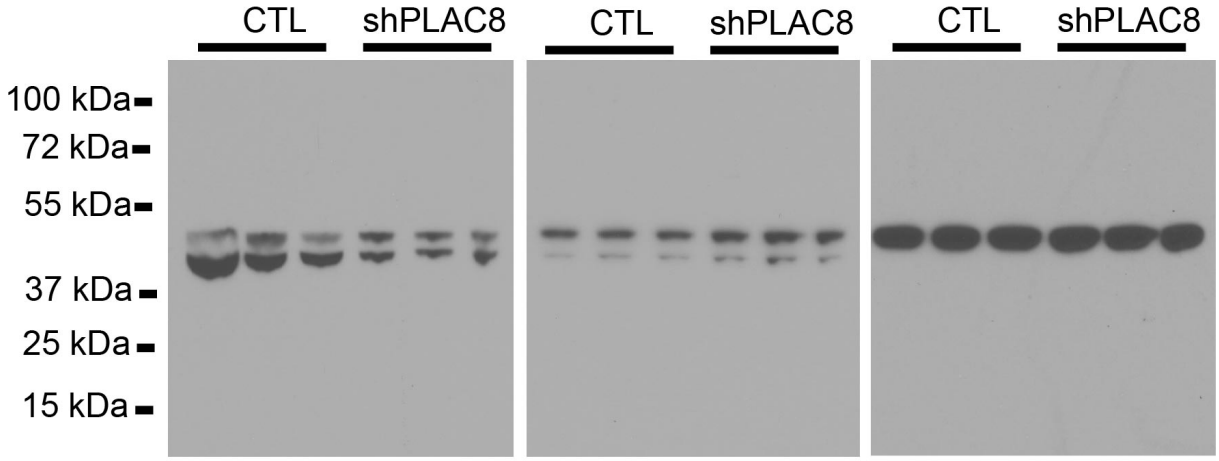

Supplemental Figure 2A PLAC8

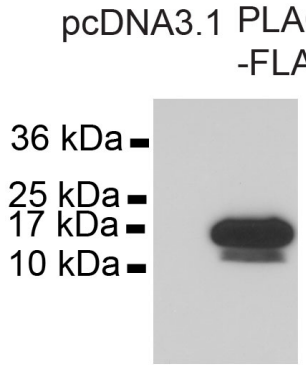

Supplemental Figure 2A FLAG

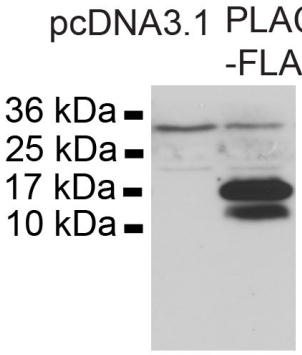

Supplemental Figure 2A TUBA

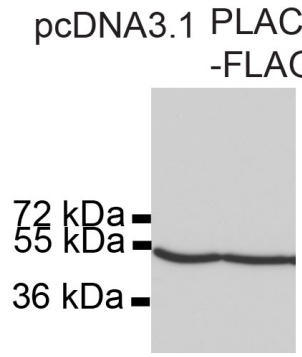

Supplemental Figure 2B PLAC8

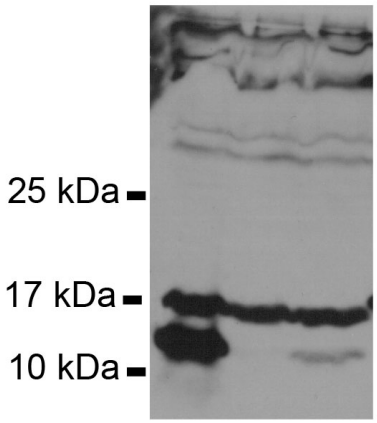

Supplemental Figure 2B TUBA

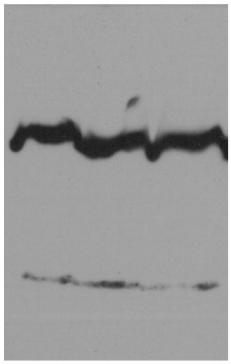

Supplemental Figure 2C Plac8.1

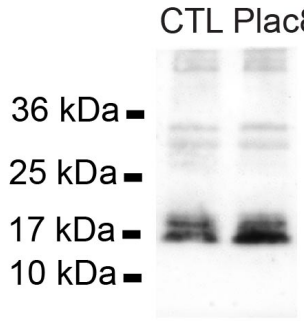

Supplemental Figure 2C HA

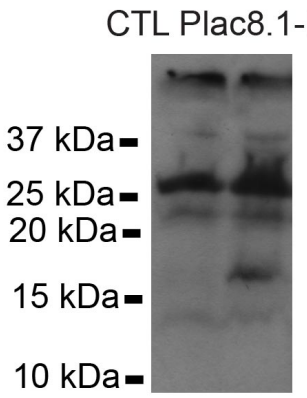

Supplemental Figure 2C Actb

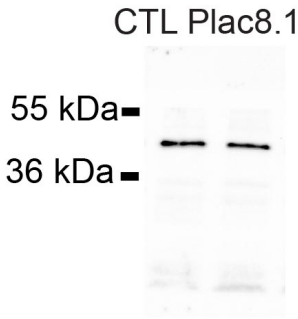

Supplemental Figure 2D PLAC8

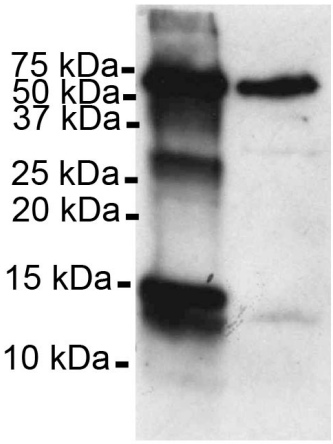

Supplemental Figure 2D Plac8.1

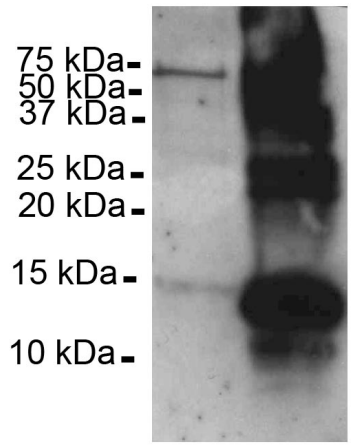

Supplemental Figure 3 PLAC8

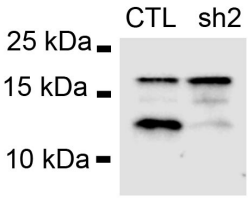

Supplemental Figure 3 ACTB

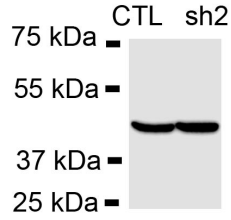

Supplemental Figure 12 p-Erk

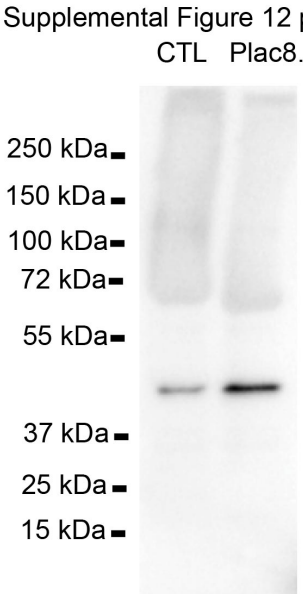

Supplemental Figure 12 Erk

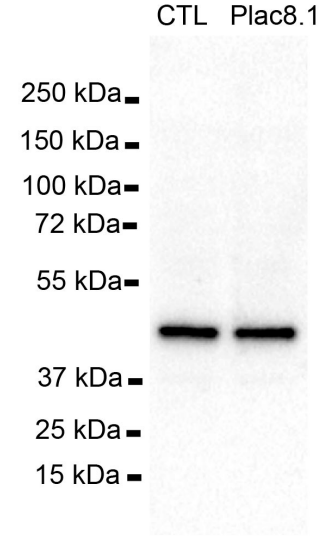

Supplemental Figure 12 p-Akt

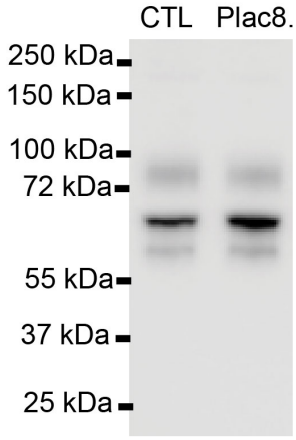

Supplemental Figure 12 Akt

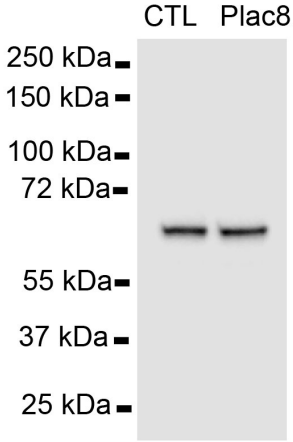

Supplemental Figure 12 Tubulin